Energy & Environmental Science

COMMUNICATION

View Article Online
View Journal | View Issue

Cite this: *Energy Environ. Sci.*, 2017, **10**, 728

Received 7th July 2016,
Accepted 18th November 2016

DOI: 10.1039/c6ee01952h

www.rsc.org/ees

Exploring the potential of a hybrid device combining solar water heating and molecular solar thermal energy storage†

Ambra Dreos,[a] Karl Börjesson,[b] Zhihang Wang,[a] Anna Roffey,[a] Zack Norwood,[c] Duncan Kushnir[d] and Kasper Moth-Poulsen*[a]

A hybrid solar energy system consisting of a molecular solar thermal energy storage system (MOST) combined with a solar water heating system (SWH) is presented. The MOST chemical energy storage system is based on norbornadiene–quadricyclane derivatives allowing for conversion of solar energy into stored chemical energy at up to 103 kJ mol^{-1} (396 kJ kg^{-1}). It is demonstrated that 1.1% of incoming solar energy can be stored in the chemical system without significantly compromising the efficiency of the solar water heating system, leading to efficiencies of combined solar water heating and solar energy storage of up to 80%. Moreover, prospects for future improvement and possible applications are discussed.

Broader context

Development of technologies for solar energy storage is a key challenge for a future society independent of fossil fuels. Hybrid solar technologies is an appealing way to overcome the limitations in current technology, and by that achieve better performing systems able to harvest and store solar energy. We present an efficient hybrid solar thermal energy storage system that combines energy storage in covalent bonds in molecular solar thermal systems with thermal energy storage in heated water. It is demonstrated that the molecular system can convert up to 1% of the incoming sunlight to storable chemical energy and at the same time, up to 80% of the incoming sunlight is transformed to heat in the water heating system. Moreover, it is shown that the chemical system can operate through more than 100 energy storage and release cycles with negligible degradation. The combined system mitigates challenges associated with both chemical and thermal energy storage and enables both long and short term energy storage.

Solutions for efficient solar energy conversion and solar energy storage are crucial for the development of a sustainable society. Technologies for conversion of solar energy into heat and electricity is seeing an impressive evolution leading to rapid integration into the energy system in several countries.[1] The most common concepts for solar energy conversion are photovoltaics (solar–electric) and solar–thermal (solar–heat). The most common photovoltaic technology is based on single junction silicon solar cells. The maximal efficiency of a single junction solar photovoltaic cell is estimated to be 32% (solar to electricity) due to spectrum losses, whereas typical efficiencies for modules today are upwards of 20%.[2] Comparatively, solar water heating systems (SWH) typically have an efficiency (solar to heat) of 20–80% depending on the application, required temperature, *etc.*[3] Such systems have found widespread use in *e.g.* water heating, district heating, industrial heating and in concentrating solar power (CSP) using heat engines for electric power production.[4] SWH systems makes use of the full solar spectrum whereas photovoltaics are limited to harvesting of photons with energies higher than the bandgap. This has led to the consideration and development of hybrid systems, as for example combined solar thermal and photovoltaic devices.[5–8]

As photovoltaics is finding more and more widespread use, technologies for mitigating challenges with intermittency and load-levelling are becoming increasingly important. In addition to electrochemical (battery) technologies, methods for storage of solar energy in chemical bonds is an attractive option since the chemical energy can be stored in a very compact way.[9] In this context, an approach is to store solar energy as latent chemical energy in photo-induced isomerization in chemical bonds, so-called molecular solar thermal (MOST).[10] In a MOST system a parent molecule is exposed to solar photons and by that converted to a high energy photoisomer; this is kinetically stable but it can isomerize back to the parent molecule and doing so it releases heat (see Fig. 1). An important parameter to

[a] *Chalmers University of Technology, Department of Chemistry and Chemical Engineering, 412 96 Gothenburg, Sweden. E-mail: kasper.moth-poulsen@chalmers.se*
[b] *Department of Chemistry and Molecular Biology, University of Gothenburg, Kemigården 4, 412 96 Gothenburg, Sweden*
[c] *Chalmers University of Technology, Department of Civil and Environmental Engineering, Building Technology, 41296 Gothenburg, Sweden*
[d] *Chalmers University of Technology, Department of Energy and Environment, Environmental Systems Analysis, 41296 Gothenburg, Sweden*

† Electronic supplementary information (ESI) available. See DOI: 10.1039/c6ee01952h

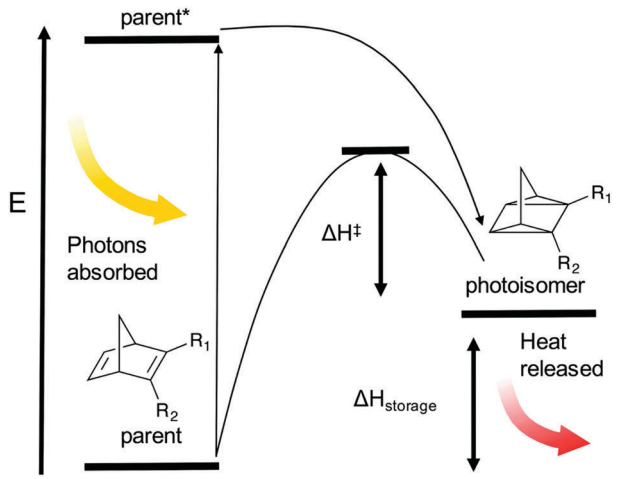

Fig. 1 Schematic representation of the norbornadiene–quadricyclane molecular solar thermal energy storage system. The energy levels are drawn to scale using values for NBD **2** where the difference between the relaxed and excited molecule corresponds to 262 kJ mol^{-1}, $\Delta H^{\ddagger}$ to 92 kJ mol^{-1}, and ΔH to 103 kJ mol^{-1}.

consider here is the quantum yield of the photoreaction (ϕ_{iso}), which is defined as in eqn (1):

$$\phi_{iso} = \frac{\text{number of isomerization events}}{\text{number of photons absorbed}} \quad (1)$$

Several systems have been explored in this context, including norbornadienes,[11–13] ruthenium compounds,[14–17] azobenzenes[18–25] and other systems;[26,27] the field has recently been reviewed.[10,28]

The focus point here is on the norbornadiene–quadricyclane system, that has shown energy storage densities up to 966 kJ kg^{-1} [29] and storage time exceeding several months.[13] The energy release can be carried out either by thermal activation[30] or by the use of catalysts.[13,31] The requirements of an efficient MOST system has been discussed several times in the literature[10,11,13,32] and can be summarized as: (i) the parent compound must absorb a significant part of the solar spectrum, (ii) the photoisomer must not compete for the absorption of sunlight, (iii) the quantum yield of the photoreaction should be 100%, (iv) the stored energy density should exceed 300 kJ kg^{-1},[33] (v) the photoisomer must be stable over extended periods of time and (vi) all reactions must proceed quantitatively, *e.g.* allows for multiple solar energy storage-release cycles. Although several systems have been greatly improved towards these requirements, no single system has fulfilled them all and thus the norbornadiene–quadricyclane system still needs optimisation to meet requirements for future applications.[34–36]

A part of the photon energy in MOST systems is needed to supply energy for the barrier preventing back conversion, at least 1.14–1.24 eV, as previously calculated by us[34] (the energy barrier is indicated as $\Delta H^{\ddagger}$ in Fig. 1). We have therefore evaluated in a previous work how these systems are expected to operate at up to 10–12% solar energy storage efficiencies (η_{MOST}), when able to absorb relatively high photon energies (1.8–1.9 eV).[34] There are two processes of energy loss in the MOST system, both resulting in heat: relaxation from the electronically excited parent molecule to the photoisomer, and ϕ_{iso} less than unity. Heating of the MOST system is in this work regarded as a pure loss.

The currently available MOST systems that are most promising in aspect of the requirements listed above operate at bandgaps in the region of 2.48–3 eV.[13,37] As a consequence, it is relevant to try to combine MOST systems with concepts for utilization of long wavelength photons. Photon upconversion has been explored as a way to improve the performance of MOST systems;[38,39] this is a very promising strategy but many challenges are still to be addressed in the development of efficient upconverting materials.[40–42]

Here we investigate for the first time a hybrid technology combining SWH and MOST, making it possible to exploit the sub-bandgap photons which the MOST systems cannot utilize. Combining SWH and MOST allows for efficient usage of low energy photons for SWH, combined with storage of the high energy photons in the form of chemical energy in the MOST system. Storage of a part of the solar energy by using the NBD-QC system can add the valuable feature of long term energy storage and on demand energy delivery to existing low or medium temperature SWH systems.

To demonstrate the effect of adding MOST based energy storage to SWH, a microfluidic hybrid device was designed (Fig. 2). The hybrid device contains two layers, with SWH in the bottom layer (dark grey) and MOST in the top layer (light grey). The upper MOST part is constituted of a fused silica microfluidic chip; it allows the high energy photons from the solar spectrum to photochemically convert norbornadiene (NBD) to quadricyclane (QC). As shown in Fig. 3a, photons with lower energy than the absorption onset of NBD, are efficiently transmitted through the upper layer of the device, and used to heat water in the lower collector, constituted of a 3D printed flow cell covered by a quartz glass slide. The front face dimensions of the device are ≈2 by 2 cm.

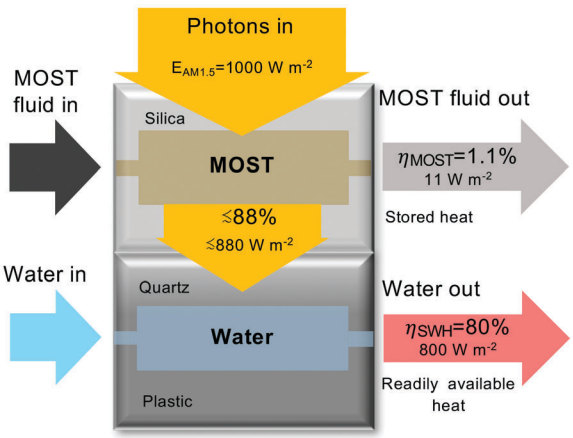

Fig. 2 Sketch of the hybrid solar energy conversion device. The upper collector is used for the conversion of the MOST system; the lower collector is used for solar water heating. Measured efficiencies are reported (NBD **2** as MOST, 0.1 M in toluene, $\dot{n}$ = 2.7 × 10^{-8} mol s^{-1}, $\dot{m}$ = 1.6 × 10^{-5} kg s^{-1}).

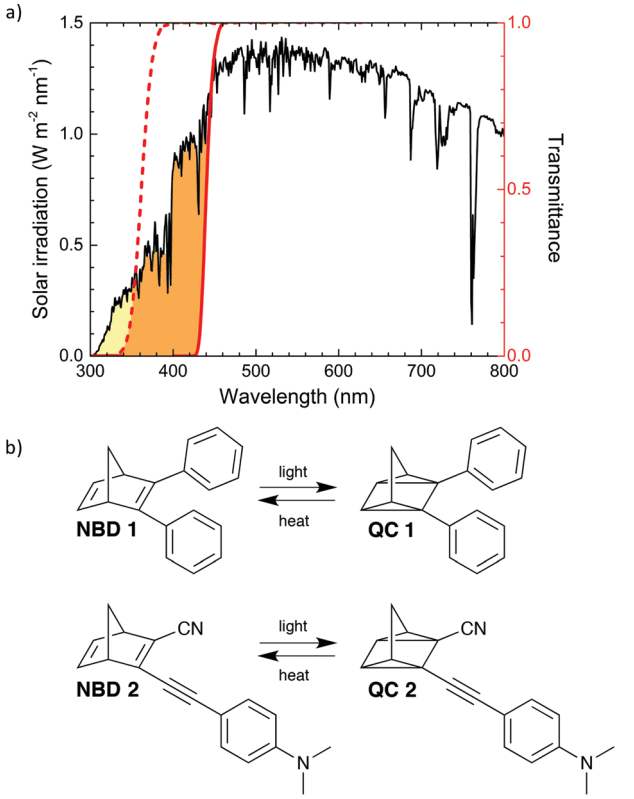

Fig. 3 (a) Spectral overlap of NBD **1** and **2** used solutions and solar spectrum in the visible range (1.5 AM); red lines indicate the transmittance of MOST, (dashed line corresponds to **1**, full line corresponds to **2**). (b) Chemical structures of compounds **1** and **2**.

The solar energy storage efficiency of the MOST system (η_{MOST}) is calculated according to eqn (2):

$$\eta_{MOST} = \frac{\dot{n}_{NBD} \cdot \alpha_{QC} \cdot \Delta H_{storage}}{A \times E_{AM1.5}} \quad (2)$$

where α_{QC} is the measured conversion of QC after irradiation, $\Delta H_{storage}$ is the stored energy of QC (in J mol^{-1}), $\dot{n}$ is the flow speed (in mol s^{-1}), A the irradiated area (in m^{-2}), and $E_{AM1.5}$ is the energy of incoming solar radiation (in W m^{-2}). To calculate the efficiency of the SWH system (η_{SWH}) eqn (3) was used:

$$\eta_{SWH} = \frac{\dot{m}_{H_2O} \cdot C_{PH_2O} \cdot \Delta T}{A \times E_{AM1.5}} \quad (3)$$

where $\dot{m}$ is the water flow-rate (in Kg s^{-1}), C_P is the heat capacity of water (J kg^{-1} K^{-1}), and ΔT is the measured temperature rise (in K). The combined efficiency of the device η_{comb} is defined as:

$$\eta_{comb} = \eta_{MOST} + \eta_{SWH} \quad (4)$$

Two norbornadienes (2,3-diphenylnorbonadiene and 2-cyano-3-((4-(dimethylamino)phenyl)ethynyl)norbornadiene, indicated as NBD **1** and NBD **2** respectively in Fig. 3b) were selected to be tested in the hybrid device. These two compounds have previously been synthesized by us, and their properties thoroughly assessed, by means of both theoretical calculations and

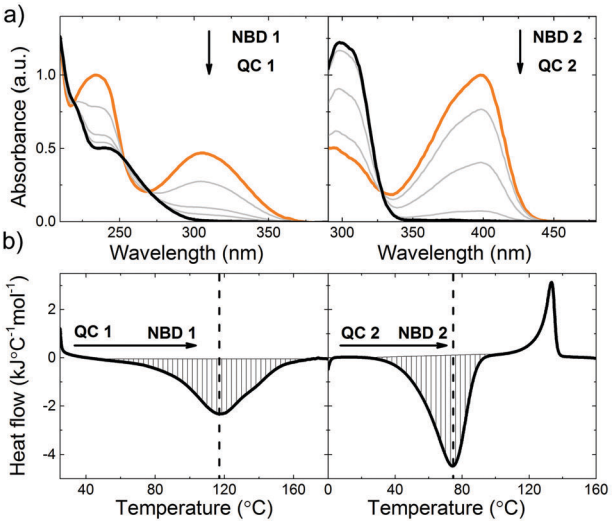

Fig. 4 (a) Stepwise photoisomerization of NBD **1** and NBD **2** (in orange) to QC **1** and QC **2** (in black).[37] (b) DSC thermogram of QC **1** and QC **2** thermally back-isomerizing to NBD **1** and NBD **2**,[37] showing the associated exothermic peak (downward, hatched). The endothermic peak (upward) associated to the melting of NBD **2** is also observed, centred at about 120 °C. Thermograms of norbornadienes are shown in the ESI.†

experimental characterization.[30,35,37,43] They both show promising features considering the requirements stated above, including complete photoswitching (see Fig. 4a), good kinetic stability of quadricyclane, high solubility (see ESI† for details) and high energy storage density, making them interesting systems for testing in a device.

NBD **1** features a photoisomerization quantum yield (ϕ_{iso}) of 60%, and a half-life of the backconversion from high energy isomer to the parent compound ($t_{1/2}$) of 42.9 days at room temperature.[30] NBD **2**, features ϕ_{iso} of 28%, and $t_{1/2}$ of 5 hours at room temperature[37] (summarised in Table 1, moreover, rate constants for QC to NBD conversion of **1** and **2** at different temperatures are reported in ESI,† Section I). The absorption onset (λ_{onset}) of **1** and **2** is 389 nm and 456 nm respectively, resulting in **2** absorbing up to 12% of the solar spectrum, compared to **1**, capable of absorbing up to 3.8%, (MOST transmittance and solar spectrum overlap are shown in Fig. 3).

The energy release associated with the thermal isomerisation of QC **1** to NBD **1** was measured using differential scanning calorimetry (DSC; Fig. 4b; see ESI† for details), while the value for **2** was recently reported.[37] **1** can store 86.5 kJ mol^{-1} (354 kJ kg^{-1}) and **2** can store 103 kJ mol^{-1} (396 kJ kg^{-1}). Assuming that the density of norbornadienes **1** and **2** are comparable to that of unsubstituted norbornadiene (906.4 g L^{-1}),[44] it is possible to calculate the volumetric energy density of **1** and **2**, which correspond to 321 kJ L^{-1} and 359 kJ L^{-1} respectively. This energy storage density of **1** and **2** can be translated to a potential temperature rise of 213 and 238 °C, respectively under adiabatic conditions. In this work **1** and **2** are dissolved in toluene (at concentrations of 70 and 100 mM respectively), in order to create a fluid system, reducing the volumetric energy density accordingly.

Table 1 Properties of the two MOST systems **1** and **2**

MOST system	λ_{max} [nm]	λ_{onset} [nm]	$t_{1/2}$	ϕ_{iso} [%]	$\Delta H_{storage}$ [kJ mol^{-1}]	η_{MOST} [%]
1	308[a]	389[a]	42.9 d[a]	60[a]	86.5	0.1[c]
2	398[b]	456[b]	5.05 h[b]	28[b]	103[b]	1.1[d]

[a] Ref. 29. [b] Ref. 31. [c] η_{MOST} calculated according to eqn (2), where **1** was dissolved in toluene (70 mM) and circulated in the device at 2 mL h^{-1}. The reported value is an average of 2 independent measurements. [d] **2** was dissolved in toluene (100 mM) and circulated in the device at 10 mL h^{-1}. The reported value is an average of 6 independent measurements.

Photoisomerization of norbornadienes **1** and **2** in solution was carried out using a solar simulator and the α_{QC} determined by ^{1}H NMR. Using eqn (2), η_{MOST} of **1** and **2** was calculated to 0.1% and 1.1%, respectively. These values are up to 2 orders of magnitude higher than our previously reported efficiencies of MOST systems in a device.[14] The improvement in the measured MOST solar energy storage efficiencies can be attributed largely to higher quantum yield of norbornadienes **1** and **2** used in this study (60% and 28% respectively) with respect to the quantum yield of the ruthenium compounds previously used (0.2%).[14,45] The fact that a part of the absorbed light is not stored is related to (1) that ϕ_{iso} is not equivalent to unity, and (2) the intrinsic property of the MOST system, which looses energy in the photoisomerization process, from the excited norbornadiene to the relaxed quadricyclane (*vide supra*). We can calculate the energy loss depending on ϕ_{iso} as E_{iso} (point 1 above):

$$E_{iso} = \int_0^{\lambda_{onset}} n_f \cdot E_f \cdot (1 - \phi_{iso}) d\lambda \quad (5)$$

where n_f is the number of photons in the solar spectrum (s^{-1} m^{-2} nm^{-1}), and E_f is the energy of each photon (J nm^{-1}). The energy loss depending on the relaxation from the electronically excited norbornadiene to the quadricyclane (point 2 above) is calculated:

$$E_{relax} = \int_0^{\lambda_{onset}} n_f \cdot \left(E_f - \frac{\Delta H_{stor}}{N_A}\right) \cdot \phi_{iso} d\lambda \quad (6)$$

where N_A is Avogadro's number. In the same way we can calculate the theoretical energy stored by a MOST system, E_{stored}, as:

$$E_{stored} = \int_0^{\lambda_{onset}} n_f \cdot \frac{\Delta H_{stor}}{N_A} \cdot \phi_{iso} d\lambda \quad (7)$$

In the case of NBD **2** it is calculate that E_{iso} = 84 W m^{-2}, E_{relax} = 21 W m^{-2}, and E_{stored} = 11 W m^{-2}. Where the latter corresponds to 1.1% of the AM1.5 solar spectrum, in accordance with η_{MOST}, the experimentally determined value. The sum of all the three contributions is equal to 117 W m^{-2}, which corresponds to the incoming solar power below 456 nm, confirming that eqn (5) and (6) are describing the main losses affecting η_{MOST}. As a consequence, increasing ϕ_{iso} to reduce E_{iso} is becoming a key parameter to improve in future works in order to reach a higher η_{MOST}.

To further evaluate the performance of the norbornadienes, the most promising compound (**2**) was subjected to a cycling test in solution (photoisomerization and subsequent thermal back-conversion) at 60 °C. As shown in Fig. 5. Compound **2** undergoes 127 cycles with negligible degradation, demonstrating excellent robustness. Additionally, the cycling test was carried out under ambient conditions (no degassing), leading to 0.2% degradation per conversion cycle (Fig. S2, ESI†) highlighting the need for an oxygen free environment to obtain negligible degradation.

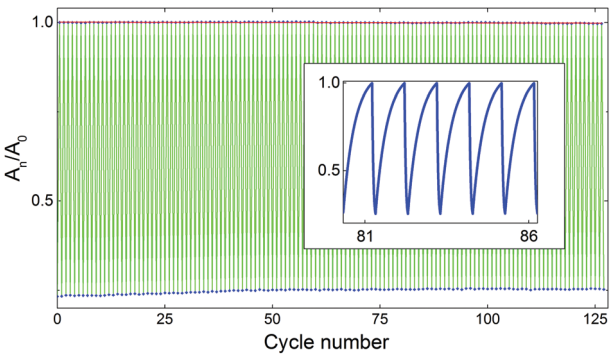

Fig. 5 Cycling tests, photoconversion followed by thermal back reaction at 60 °C for 127 cycles. The normalized absorption (a.u.) of the solution of **2** after each half cycle of thermal back-conversion and photoisomerization is reported. The inset shows a detail of the normalised absorption (a.u.) of cycles 81 to 86.

The performance of the SWH collector was assessed in four different working conditions. Water was circulated at different flow-rates ($\dot{m}$) in the lower collector, while in the upper collector circulated air, toluene or solutions of **1** or **2** in toluene. The water temperature increase (ΔT) in the SWH collector was measured by monitoring the temperature before (T_1) and after (T_2) exposure to simulated sunlight and η_{SWH} was calculated according to eqn (3). The concentration of **1** or **2** were chosen in order to maintain transmission through the upper collector near zero below λ_{onset}. In this way the MOST layer is acting as a cut-off filter below the onset of absorption. However, a significant part of the solar photons, those with lower energy than λ_{onset}, is still available for water heating after being transmitted through the upper collector (as can be seen in Fig. 2).

Fig. 6 show measured temperature rises over the SWH collector (ΔT), recorded at different water flow-rates. The observed ΔT is between 8 °C and 17 °C, with calculated η_{SWH} between 47% and 82%. In the presented device, adding toluene or a solution of MOST in the upper layer of the collector does not significantly affect the measured ΔT of the water and thus η_{SWH} of the SWH device. While using MOST **1** or **2** to store the energy it is still possible to reach values of η_{SWH} up to 80%.

An energy balance equation for the full spectrum can therefore be defined as:

$$E_{AM1.5} = (\eta_{SWH} + \eta_{MOST}) \cdot E_{AM1.5} + E_{iso} + E_{relax} + E_{th} \quad (8)$$

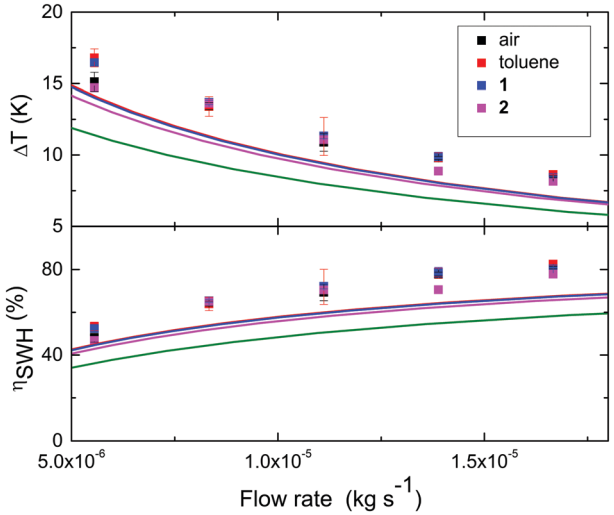

Fig. 6 Increase of water temperature and η_{SWH} at different flow rates. In the upper collector air (black), toluene (red) or NBD **1** (blue) or **2** (pink) in toluene were circulated; errors as standard deviations are reported for the measurements done while in the upper collector is circulating air, toluene or **1**. The measured points are compared with the simulated values for the device (solid lines, red for toluene in the upper collector, blue for NBD **1**, and pink for NBD **2**). The device operating with an optimized MOST system with cut off at 590 nm is also simulated (green line). For details of simulations see ESI.†

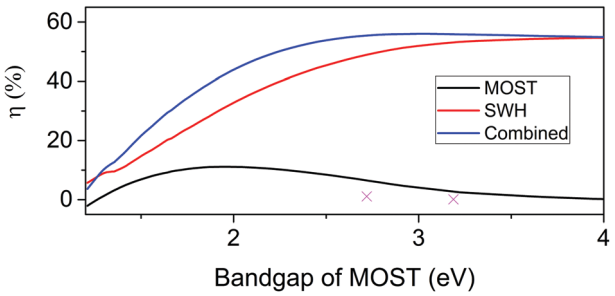

Fig. 7 Simulated solar water heating (red), molecular solar thermal (black), as well as combined efficiencies (blue) as a function of bandgap of the molecular solar thermal system. The simulation was done using a flow rate of 8.3×10^{-5} kg s^{-1}; the experimental values of compounds **1** and **2** are marked with a cross.

where E_{th} are the thermal energy losses, which correspond to 8% of the incoming solar radiation at a flow speed of $\dot{m} = 1.6 \times 10^{-5}$ kg s^{-1}.

The above described experiments demonstrate that it is possible to capture and store part of the high energy photons in a MOST system without severely compromising the SWH efficiency. To validate and extrapolate these results, the thermal behaviour of the hybrid device was simulated. The basis of the simulation was a parametric analysis of a coupled MOST and SWH system (see ESI† for details), in analogue to the coupled PV/SWH simulations by Norwood *et al.*,[46] Otanicar *et al.*[47] and Zondag *et al.*[48] A MatLab script was developed to solve the coupled mass and heat transfer equations using the Newton–Raphsons method (see ESI† for details). The solid lines in Fig. 6 show simulated values of temperature rises and η_{SWH} of a SWH device having an incorporated MOST system (Fig. S4, ESI†). The results from the simulation follows the experimental trends, although with a general decrease in ΔT and η_{SWH}. Using existing MOST systems, which have relatively low onsets of absorption (389 nm and 456 nm respectively, corresponding to 3.4 eV and 2.8 eV), only minor decreases in the generated heat of the SWH system is experienced. This is rationalized by the relatively low amount of solar flux in the UV/blue part of the solar spectra which is absorbed by the MOST (12% in the case of NBD **2**). If instead an optimized MOST system, having a bandgap of 2.1 eV (as defined in previous work by us[34]), was used, a 13% decrease in η_{SWH} is expected based on the simulation. However, a MOST system with a bandgap of 2.1 is expected to be able to harvest and store 9.9% of the solar energy in chemical bonds for on demand delivery.[34] The performed simulations validate the experimental results, and leads to a high combined efficiency η_{comb} of a hybrid device that uses an optimal bandgap MOST system. Fig. 7 show how η_{MOST} and η_{SWH} varies with the bandgap of the MOST system. With lowering bandgap, the solar energy storage efficiency of the MOST system increases until a maximum point at around 2 eV. At the same time the SWH efficiency decreases. However, in combination the decreased SWH efficiency is balanced by an increase in the MOST solar energy storage efficiency. It should noted that at high MOST bandgaps, η_{comb} is decreasing. This because the MOST system is absorbing the majority of photon energy but at the same time $\Delta H_{storage}$ decrease towards zero, resulting in heating of the MOST system, which we here regard as an energy loss.

As is the case with any new technology, initial applications will be in niches where MOST offers unique technical properties and where cost-per-joule is of lesser importance. Because a portion of energy in the MOST system is stored in chemical bonds, the potential exists for very stable long-term storage limited by the volume of the storage capacity. This energy can be transported and delivered in very precise amounts with high reliability. An interesting contribution in this context is the review by Kucharski *et al.*[10] where MOST technologies are thoroughly analysed and put into context by comparing them with other heat batteries. They as well discuss how MOST solar thermal batteries could be useful in some niches applications as discussed in our work (*e.g.* off grids stations, extreme environments like deserts, heating of water for disinfection and cooking).

Another example of a possible application could be satellite thermal control systems. Here the system might run best without the SWH system for instance, collecting solar energy exclusively in the chemical bonds of the MOST system for use as a thermal buffer that can be renewably regenerated. Design drivers for satellite thermal storage systems heavily emphasize precision controllability, reliability and, to a lesser degree, energy storage density.[49] The MOST system described here has reached a performance level where it has some technical advantages over common solutions such as fluid cooling and phase change materials (PCMs), namely that it works over a range of temperatures and has the ability to produce a controlled temperature rise as well as actively transport heat.

The demonstrated technical performance of the system 397 kJ kg^{-1} = 110 W h kg^{-1} (present compounds), with a potential of 966 kJ kg^{-1} = 268 W h kg^{-1} (unsubstituted norbornadiene)[29] is very competitive with modern lithium ion battery chemistries for energy density, indicating that it may be a viable technique in any application that uses battery energy for resistive heating. It also exceeds the enthalpy of fusion for most common PCMs (*e.g.* paraffin waxes at 200–270 kJ kg^{-1}). The MOST system can thus also be competitive from a gravimetric energy density standpoint. The system as described thus represents an advance to the point where MOST is a technically interesting solution in some applications. Future work along these lines should produce prototypes that can empirically demonstrate real world performance and reliability and begin to shed light on system costs. The strong cyclability performance of the system as demonstrated is one essential prerequisite for applications demanding reliability in harsh or remote environments, as well as for systems that are energy efficient in a full lifecycle sense.

If such prerequisites are met, the potential to release heat at up to 238 °C indicates that applications may extend beyond what is possible with water based heat storage. Such applications include pre-warming of stand-alone systems that require heat on startup below certain temperatures (*e.g.* pumps or engines), but which might be located in remote locations or harsh environments without access to full-time power (or steady sunlight) and where high logistics cost of delivered fuel enhances the competitiveness of renewable approaches. Of course, the additional need for SWH under the sunlight hours would greatly enhance the applicability of the MOST technology.

Any future larger scale application of MOST technology faces two primary challenges, which together can form a roadmap for long term research and development. The first challenge to overcome for further development of such thermochemical storage technologies is likely the toxicity of the solvent; reduction in the toxicity, or elimination of the solvent as demonstrated for azobenzenes by Kimizuka and co-workers[24,50] would open up many more potential applications such as portable cooking devices that can be recharged with sunlight and can cook when the sun is down.

Lastly, reduction of cost through mass production of the constituent chemicals is certainly needed before such systems could compete with other solar renewable technologies in bulk energy applications. Space heating, with storage from day to night, for instance would be a very challenging application area given the maturity of other technologies in that field. The old analysis of Philippopoulous *et al.*[51] is still largely correct in that it may be impossible for the MOST system by itself to reach cost competitive generation of bulk steam, although the current system does represent a significant advance towards the optimal end of the parameter space they used. Their economic analysis explicitly did not include MOST as a marginal source in combination with other solar approaches, however the hybrid concept is mentioned in their outlooks section. We have demonstrated here that such a hybridized approach is achievable technically while maintaining high efficiency of the device, which is one critical step towards being able to re-evaluate the technology. Complete economic analysis of such a system is well beyond the remit of this paper. Breaking through the barrier for commercialization in a very competitive solar landscape would be a significant and difficult challenge, but breakthroughs are likely happening, given the relative youth of solar technologies and the current worldwide trend to phase out fossil fuels.

Conclusions

A new concept in the form of a hybrid technology, combining solar water heating and molecular solar thermal energy storage has been presented, and a device fabricated. Two norbornadienes (**1** and **2** in Fig. 3) have been selected to be tested in the device, and their robustness tested through cyclability experiments, which showed negligible degradation over more than 100 cycles. The energy storage efficiency of the molecular solar thermal system, η_{MOST}, is up to 1.1%, representing a major step forward compared to previously reported MOST efficiencies in devices.[14] The efficiency of the solar water heating part, η_{SWH}, is measured to be up to 80%.

Main areas where to focus future efforts to improve the hybrid technology and generically a MOST technology, are identified as: improved quantum yield of photoisomerization ϕ_{iso}, half life of quadricyclane, $t_{1/2}$, and developing a solvent free, liquid MOST system.

Acknowledgements

The authors would like to thank the Swedish Research Council, Knut & Alice Wallenberg Foundation and the Swedish foundation for strategic research for financial support. A. Lennartson and M. Quant are acknowledged for the synthesis of compounds **1** and **2**.

Notes and references

1 IEA International Energy Agency, *TRENDS 2015 In Photovoltaic Applications*, 2015.
2 W. Shockley and H. J. Queisser, *J. Appl. Phys.*, 1961, **32**, 510–519.
3 S. A. Kalogirou, *Solar thermal collectors and applications*, 2004, vol. 30.
4 F. Mauthner, W. Weiss and M. Spork-Dur, *Solar Heat Worldwide*, 2015.
5 F. Sarhaddi, S. Farahat, H. Ajam, A. Behzadmehr and M. M. Adeli, *Appl. Energy*, 2010, **87**, 2328–2339.
6 O. Zogou and H. Stapountzis, *Appl. Energy*, 2012, **91**, 103–115.
7 P. Bermel, K. Yazawa, J. L. Gray, X. Xu and A. Shakouri, *Energy Environ. Sci.*, 2016, 2776–2788.
8 H. R. Seyf and A. Henry, *Energy Environ. Sci.*, 2654, **9**, 2654–2665.
9 N. S. Lewis and D. G. Nocera, *Proc. Natl. Acad. Sci. U. S. A.*, 2006, **103**, 15729–15735.
10 T. J. Kucharski, Y. Tian, S. Akbulatov and R. Boulatov, *Energy Environ. Sci.*, 2011, **4**, 4449–4472.

11 Z. Yoshida, *J. Photochem.*, 1985, **29**, 27–40.
12 V. I. Minkin, V. A. Breit, V. A. Cherwoivanov, A. D. Dubonosov and S. V. Galichev, *Mol. Cryst. Liq. Cryst. Sci. Technol., Sect. A*, 1994, **246**, 151–154.
13 A. D. Dubonosov, V. A. Bren and V. A. Chernoivanov, *Russ. Chem. Rev.*, 2002, **71**, 917–927.
14 K. Moth-Poulsen, D. Ćoso, K. Börjesson, N. Vinokurov, S. K. Meier, A. Majumdar, K. P. C. Vollhardt and R. A. Segalman, *Energy Environ. Sci.*, 2012, **5**, 8534–8537.
15 Y. Kanai, V. Srinivasan, S. K. Meier, K. P. C. Vollhardt and J. C. Grossman, *Angew. Chem., Int. Ed.*, 2010, **49**, 8926–8929.
16 R. Boese, J. K. Cammack, A. J. Matzger, K. Pflug, W. B. Tolman, K. P. C. Vollhardt and T. W. Weidman, *J. Am. Chem. Soc.*, 1997, **119**, 6757–6773.
17 M. R. Harpham, S. C. Nguyen, Z. Hou, J. C. Grossman, C. B. Harris, M. W. Mara, A. B. Stickrath, Y. Kanai, A. M. Kolpak, D. Lee, D. J. Liu, J. P. Lomont, K. Moth-Poulsen, N. Vinokurov, L. X. Chen and K. P. C. Vollhardt, *Angew. Chem., Int. Ed.*, 2012, **51**, 7692–7696.
18 A. M. Kolpak and J. C. Grossman, *Nano Lett.*, 2011, **11**, 3156–3162.
19 Y. Feng, H. Liu, W. Luo, E. Liu, N. Zhao, K. Yoshino and W. Feng, *Sci. Rep.*, 2013, **3**, 3260.
20 W. Feng, W. Luo and Y. Feng, *Nanoscale*, 2012, **4**, 6118–6134.
21 T. J. Kucharski, N. Ferralis, A. M. Kolpak, J. O. Zheng, D. G. Nocera and J. C. Grossman, *Nat. Chem.*, 2014, **6**, 441–447.
22 A. M. Kolpak and J. C. Grossman, *J. Chem. Phys.*, 2013, **138**, 34303.
23 D. Zhitomirsky, E. Cho and J. C. Grossman, *Adv. Energy Mater.*, 2016, **6**, 1502006.
24 K. Masutani, M. Morikawa and N. Kimizuka, *Chem. Commun.*, 2014, **50**, 15803–15806.
25 D. Zhitomirsky and J. C. Grossman, *ACS Appl. Mater. Interfaces*, 2016, **8**, 26319–26325.
26 M. Cacciarini, A. B. Skov, M. Jevric, A. S. Hansen, J. Elm, H. G. Kjaergaard, K. V. Mikkelsen and M. Brøndsted Nielsen, *Chem. – Eur. J.*, 2015, **21**, 7454–7461.
27 M. Blanco-Lomas, D. Martínez-López, P. J. Campos and D. Sampedro, *Tetrahedron Lett.*, 2014, **55**, 3361–3364.
28 A. Lennartson, A. Roffey and K. Moth-Poulsen, *Tetrahedron Lett.*, 2015, **56**, 1457–1465.
29 X. An and Y. Xie, *Thermochim. Acta*, 1993, **220**, 17–25.
30 V. Gray, A. Lennartson, P. Ratanalert, K. Börjesson, K. Moth-Poulsen and B. Karl, *Chem. Commun.*, 2014, **50**, 5330–5332.
31 S. Miki, T. Maruyama, T. Ohno, T. Tohma, S. Toyama and Z. Yoshida, *Chem. Lett.*, 1988, 861.
32 K. Moth-Poulsen, *Organic Synthesis and Molecular Engineering*, 2014, pp. 179–196.
33 V. A. Bren', A. D. Dubonosov, V. I. Minkin and V. A. Chernoivanov, *Russ. Chem. Rev.*, 1991, **60**, 913–948.
34 K. Börjesson, A. Lennartson and K. Moth-Poulsen, *ACS Sustainable Chem. Eng.*, 2013, **1**, 585–590.
35 M. J. Kuisma, A. M. Lundin, K. Moth-Poulsen, P. Hyldgaard and P. Erhart, *J. Phys. Chem. C*, 2016, **120**, 3635–3645.
36 O. Brummel, D. Besold, T. Döpper, Y. Wu, S. Bochmann, F. Lazzari, F. Waidhas, U. Bauer, P. Bachmann, C. Papp, H. P. Steinrück, A. Görling, J. Libuda and J. Bachmann, *ChemSusChem*, 2016, **9**, 1424–1432.
37 M. Quant, A. Lennartson, A. Dreos, M. Kuisma, P. Erhart, K. Börjesson and K. Moth-Poulsen, *Chem. – Eur. J.*, 2016, **22**, 13265–13274.
38 K. Börjesson, D. Dzebo, B. Albinsson and K. Moth-Poulsen, *J. Mater. Chem. A*, 2013, **1**, 8499–8680.
39 N. Kimizuka, N. Yanai and M. Morikawa, *Langmuir*, 2016, DOI: 10.1021/acs.langmuir.6b03363.
40 V. Gray, D. Dzebo, M. Abrahamsson, B. Albinsson and K. Moth-Poulsen, *Phys. Chem. Chem. Phys.*, 2014, **16**, 10345–10352.
41 T. F. Schulze and T. W. Schmidt, *Energy Environ. Sci.*, 2015, **8**, 103–125.
42 K. Börjesson, P. Rudquist, V. Gray and K. Moth-Poulsen, *Nat. Commun.*, 2016, **7**, 12689.
43 M. Kuisma, A. Lundin, K. Moth-Poulsen, P. Hyldgaard and P. Erhart, *ChemSusChem*, 2016, **9**, 1786–1794.
44 N. A. Belikova, L. G. Vol'fson, K. V. Kuznetsova, N. N. Mel'nikov, A. I. Person, A. F. Plate and M. A. Pryanishnikova, *Zh. Prikl. Khim.*, 1960, **33**, 454–463.
45 A. Lennartson, A. Lundin, K. Börjesson, V. Gray and K. Moth-Poulsen, *Dalton Trans.*, 2016, 8740–8744.
46 Z. Norwood, E. Nyholm, T. Otanicar and F. Johnsson, *PLoS One*, 2014, **9**, 1–31.
47 T. Otanicar, I. Chowdhury, P. E. Phelan and R. Prasher, *J. Appl. Phys.*, 2010, **108**, 1–9.
48 H. A. Zondag, D. W. de Vries, W. G. J. van Helden, R. J. C. van Zolingen and A. A. van Steenhoven, *Sol. Energy*, 2003, **74**, 253–269.
49 T. D. Swanson and G. C. Birur, *Appl. Therm. Eng.*, 2003, **23**, 1055–1065.
50 K. Ishiba, M. A. Morikawa, C. Chikara, T. Yamada, K. Iwase, M. Kawakita and N. Kimizuka, *Angew. Chem., Int. Ed.*, 2015, **54**, 1532–1536.
51 C. Philippopoulos, D. D. Economou, C. C. Economou, J. Marangozis, C. Phlllppopoulos and J. Marangoris, *Ind. Eng. Chem. Prod. Res. Dev.*, 1983, **22**, 627–633.

